Inorganic Chemistry

Article

pubs.acs.org/IC

Decaborane Thiols as Building Blocks for Self-Assembled Monolayers on Metal Surfaces

Jonathan Bould,*[,†] Jan Macháček,[†] Michael G. S. Londesborough,[†] Ramón Macías,[‡] John D. Kennedy,[†,§] Zdeněk Bastl,[⊥] Patrick Rupper,[∥] and Tomáš Baše*[,†]

[†]Institute of Inorganic Chemistry, v.v.i., Academy of Sciences of the Czech Republic, 250 68 Husinec-Řež, Czech Republic

[‡]Instituto Universitario de Catálisis Homogénea, Universidad de Zaragoza, 50009-Zaragoza, Spain

[§]The School of Chemistry, University of Leeds, Leeds LS2 9JT, U.K.

[⊥]J. Heyrovský Institute of Physical Chemistry, v.v.i., Academy of Sciences of the Czech Republic, Dolejškova 3, 182 23 Prague 8, Czech Republic

[∥]Laboratory for Advanced Fibers, Empa, Swiss Federal Laboratories for Materials Science and Technology, Lerchenfeldstrasse 5, 9014 St. Gallen, Switzerland

Supporting Information

ABSTRACT: Three *nido*-decaborane thiol cluster compounds, [1-(HS)-*nido*-$B_{10}H_{13}$] **1**, [2-(HS)-*nido*-$B_{10}H_{13}$] **2**, and [1,2-$(HS)_2$-*nido*-$B_{10}H_{12}$] **3** have been characterized using NMR spectroscopy, single-crystal X-ray diffraction analysis, and quantum-chemical calculations. In the solid state, **1**, **2**, and **3** feature weak intermolecular hydrogen bonding between the sulfur atom and the relatively positive bridging hydrogen atoms on the open face of an adjacent cluster. Density functional theory (DFT) calculations show that the value of the interaction energy is approximately proportional to the number of hydrogen atoms involved in the interaction and that these values are consistent with a related bridging-hydrogen atom interaction calculated for a $B_{18}H_{22}\cdot C_6H_6$ solvate. Self-assembled monolayers (SAMs) of **1**, **2**, and **3** on gold and silver surfaces have been prepared and characterized using X-ray photoelectron spectroscopy. The variations in the measured sulfur binding energies, as thiolates on the surface, correlate with the (CC2) calculated atomic charge for the relevant boron vertices and for the associated sulfur substituents for the parent $B_{10}H_{13}$(SH) compounds. The calculated charges also correlate with the measured and DFT-calculated thiol ^{1}H chemical shifts. Wetting-angle measurements indicate that the hydrophilic open face of the cluster is directed upward from the substrate surface, allowing the bridging hydrogen atoms to exhibit a similar reactivity to that of the bulk compound. Thus, [$PtMe_2(PMe_2Ph)_2$] reacts with the exposed and acidic B−H−B bridging hydrogen atoms of a SAM of **1** on a gold substrate, affording the addition of the metal moiety to the cluster. The XPS-derived stoichiometry is very similar to that for a SAM produced directly from the adsorption of [1-(HS)-7,7-$(PMe_2Ph)_2$-*nido*-7-$PtB_{10}H_{11}$] **4**. The use of reactive boron hydride SAMs as templates on which further chemistry may be carried out is unprecedented, and the principle may be extended to other binary boron hydride clusters.

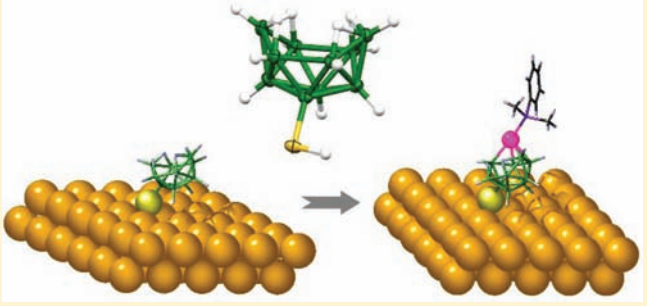

INTRODUCTION

Self-assembled monolayers (SAMs) represent *quasi*-crystalline two-dimensional interfaces that are useful for tuning various physical properties of substrate surfaces according to requirements. The further modification of the molecules held as self-assembled monolayers is of interest in the context of a general effort to understand materials on a molecular level, and also to use single molecules as fundamental building blocks for producing bottom-up surface assemblies with tailored physicochemical properties and composition.[1] The most common two-dimensional assemblies comprise organic molecules tethered to either a gold or a silver substrate by a thiol {-SH} anchoring group.[2] Recently in this context, cage molecules have started to attract special attention because of their rigid three-dimensional architectures and their suitability for structural and chemical modification.[3] 1,2-Dicarba-*closo*-dodecaboranes, with their icosahedral molecular structures, are representatives of inorganic cluster molecules belonging to this category. Since the first report of their use as {SH}-derivatized components of monolayer-protected colloids and self-assembled monolayers in 2005,[4] they have been shown to possess several unique features compared to their organic counterparts, such as a higher stability against heating and chemical substitution.[5] These features have made them potentially superior candidates for the molecular protection of silver surfaces.[6] Their large dipole

Received: September 12, 2011
Published: January 9, 2012

   dx.doi.org/10.1021/ic202000b | *Inorg. Chem.* 2012, 51, 1685−1694

moments have also been used to explore changes in the work-function of gold and silver flat surfaces that have been modified with differently orientated dicarba-*closo*-dodecaborane dipoles.[6,7]

Nido-decaborane thiols[8] constitute a further group of borane cluster compounds that are potentially suitable as surface modifiers, and we have become interested in investigating this class of compounds for a number of reasons. First, in contrast to the dicarba-*closo*-dodecaboranyl clusters, a *nido*-decaboranyl cluster possesses a hexagonal boat-shaped open face containing four acidic bridging hydrogen atoms. SAMs of these molecules are, therefore, potential inorganic building blocks for further chemistry on a self-assembled surface and in this they complement the predominance of the use of organic groups in the chemical modification of surfaces.[1b] Second, the *nido*-decaboranyl framework is the starting point for the synthesis of monometallaundecaborane clusters such as $[(PMe_2Ph)_2MB_{10}H_{12}]$ (where M = Pt or Pd), from which bimetalladodecaborane clusters, $[(PMe_2Ph)_4M_2B_{10}H_{10}]$, may then be constructed.[9] In solution, these bimetalladodecaborane compounds have the ability to reversibly sequester small molecules such as O_2, CO, and SO_2 across the metal−metal vector. The process is accompanied by a marked color change.[9b] In addition to mild warming or purging with an inert gas, the sequestered molecules can be ejected under UV irradiation, producing, for example, O_2 in the excited singlet state.[10] We are therefore interested in examining the ability of these compounds, both in solution and as self-assembled monolayers, to act as chemical sensors or as potentially reactive nanoscale surfaces.

In this study, we report on three *nido*-decaborane thiols, [1-(HS)-*nido*-$B_{10}H_{13}$] **1**, [2-(HS)-*nido*-$B_{10}H_{13}$] **2**, and [1,2-$(HS)_2$-*nido*-$B_{10}H_{12}$] **3**, and on their self-assembly and immobilization as monolayers on gold and silver surfaces. In particular we investigate their attachment to the surface via two different thiol-substituted cluster vertices. SAMs of these compounds on both gold and silver surfaces are characterized using X-ray photoelectron spectroscopy (XPS) and contact-angle measurements. We also show here the synthesis and characterization of the monometallaborane thiols, [1-(HS)-7,7-$(PMe_2Ph)_2$-*nido*-7-$PtB_{10}H_{11}$] **4** and [4-(HS)-7,7-$(PMe_2Ph)_2$-*nido*-7-$PtB_{10}H_{11}$] **5**, and, within the context of this manuscript, we provide a fundamental characterization of these nonvolatile species together with a discussion of their analysis using XPS. They also constitute the first step along the synthetic pathway of a logical continuation toward our target of constructing SAMs composed of bimetallaboranes that can reversibly sequester small gas molecules. The compounds are also characterized by multinuclear NMR spectroscopy, and by single-crystal X-ray diffraction analyses for molecular structure determination.

RESULTS AND DISCUSSION

Synthesis, NMR Spectroscopic and Crystallographic Characterization. The decaborane thiol cluster compounds [1-(HS)-*nido*-$B_{10}H_{13}$] **1**, and [2-(HS)-*nido*-$B_{10}H_{13}$] **2** were synthesized from *nido*-$B_{10}H_{14}$, elemental sulfur, and $AlCl_3$ at 120 °C. They were first reported in 1979 but the products were not fully characterized.[8] The original reported NMR data for **1** and **2** were limited to the chemical shift values of the thiol-substituted boron vertices and of the thiol proton. During our preparation of **1** and **2**, we obtained a small amount of a new decaborane dithiol [1,2-$(HS)_2$-*nido*-$B_{10}H_{12}$] **3** from the residues produced during the crystallization of **2** (Scheme 1). We have

Scheme 1. Synthesis of Thiolated Decaboranes

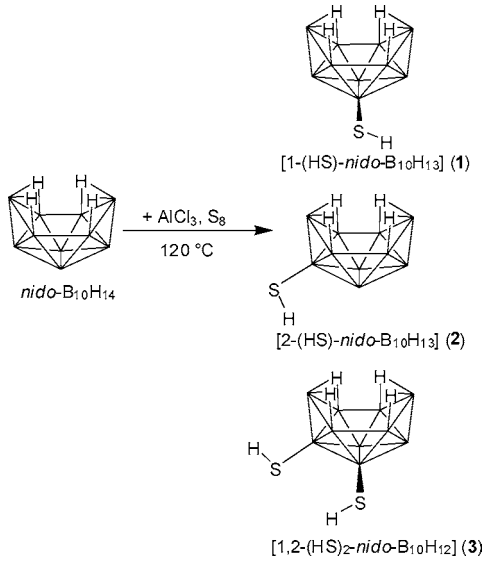

now obtained full ^{11}B and ^{1}H NMR data on the three compounds, and, together with the aid of GIAO shielding calculations via density-functional theory (DFT) using the B3LYP/6-31G* methodology and basis set,[11] we have assigned all the ^{11}B and ^{1}H resonances to their respective cluster positions (Table 1). It may be noted that the measured thiol proton chemical shift in **2** of +0.12 ppm considerably differs from the value of +1.21 ppm reported in the original paper (both in $CDCl_3$). In the ^{1}H NMR experiments, we carried out selective ^{11}B irradiation of the singlet boron resonances associated with the atoms bearing the thiol substituents: this procedure resulted in a clear sharpening of the thiol proton resonance by the removal of the coupling from ^{2}J (^{11}B-S-^{1}H), enabling its definitive identification and assignment. Interestingly, the trends in measured chemical shift values for the thiol protons in compounds **1** to **3**, as well as in their metallaborane derivatives **4** and **5** described below, match the calculated values quite well at this level of calculation.

Single-crystal X-ray diffraction studies of the three decaborane thiol compounds **1** to **3** established the positions of all the heavy atoms in the molecules. All cluster hydrogen atoms were apparent in the residual electron-density map after anisotropic refinement of the heavier atoms. For the thiol hydrogen atoms, the remaining highest electron-density peak, after isotropic hydrogen atom refinement, was close to the sulfur atoms, but final refinement was carried out using a riding model. Drawings of the molecular structures are shown in Figure 1.

A comparison of the interatomic dimensions for **1**−**3** reveals that the clusters do not suffer significant changes in their interatomic separations because of the presence of the thiol substituents. The main differences appear in the B(5)−B(10)/B(7)−B(8) and the B(1)−B(3) distances. In **2**, which contains an idealized mirror plane parallel to B(5)−B(10) and to B(7)−B(8), these distances are very similar at 1.961(2) and 1.976(2) Å, respectively [cf. 2.01(2) Å in unsubstituted $B_{10}H_{14}$].[12] But in **1**, the B(7)−B(8) distance, which is the one distal to the B(1)−SH linkage, is significantly longer at 2.001(2) Å, compared to the B(5)−B(10) vector at 1.961(2) which is adjacent to the thiol substituent, and this effect of the S(1) substituent is also seen in **3** (2.006(3) and 1.971(3) Å respectively). The only other dimensions of note in **1** and **3** are the B(1)−B(3) distances of

dx.doi.org/10.1021/ic202000b | Inorg. Chem. 2012, 51, 1685−1694

Table 1. Measured ^{11}B and ^{1}H NMR Chemical Shift Data for Compounds [1-(HS)-*nido*-$B_{10}H_{13}$] 1, [2-(HS)-*nido*-$B_{10}H_{13}$] 2, and [1,2-$(HS)_2$-*nido*-$B_{10}H_{13}$] 3[a]

1			2			3		
assign.	$\delta(^{11}B)$	$\delta(^{1}H)$	assign.	$\delta(^{11}B)$	$\delta(^{1}H)$	assign.	$\delta(^{11}B)$	$\delta(^{1}H)$
1	+21.2[+23.6]	*b*	1, 3	+13.9[+12.5]	+3.91	1	+21.5[+23.5]	*b*
3	+15.7[+15.5]	+4.14	6	+10.1[+5.9]	+4.10	3	+17.2[+15.3]	+4.09
6, 9	+7.7[+4.3]	+3.78	9	+7.7[+5.8]	+3.81	6	+7.6[+3.6]	+4.05
5, 10	+3.2[+2.6]	+3.15	5, 7	+1.8[+1.8]	+3.46	9	+5.2[+1.8]	+3.74
7, 8	−1.1[−2.5]	+3.26	8, 10	+0.6[−0.4]	+3.02	7	+3.0[+1.4]	+3.39
2, 4	−34.4[−36.8]	+0.69	2	−25.4[−23.5]	*b*	8	+1.3[+0.7]	+3.09
			4	−35.4[−36.5]	+0.79	5	−0.4[−1.6]	+3.29
						10	−0.8[−2.5]	+3.38
						2	−25.0[−23.0]	*b*
						4	−34.4[−36.3]	+0.83
S-*H* (1)		+1.49[c]	S-*H*(2)		+0.12[d]	S-*H* (2/1)		+0.18, +1.93[e]
		[+1.92]			[−0.7]			[+0.18], [+2.7]
μ-(5,6; 101)		−1.55[−2.08]	*μ*-(6,7; 8,9)		−2.09[−2.69]			−1.02, −1.55
μ-(101; 8,9)		−2.05[−2.66]	*μ*-(5,6; 101)		−1.46[−2.07]			−1.40, −2.06

[a]In $CDCl_3$ solution at 300 K B3LYP/6-31G with DFT-calculated shielding data in [square brackets]. [b]Thiol substituent position. [c]Sharpens on ^{1}H-{^{11}B selective} irradiation at $\delta(^{11}B)$ +21.2 ppm. [d]Sharpens on ^{1}H-{^{11}B selective} irradiation at δ (^{11}B) +25.4 ppm. [e]Resonances selectively sharpen on ^{1}H-{^{11}B selective} irradiation at $\delta(^{11}B)$ +21.5 and −25.0 ppm respectively.

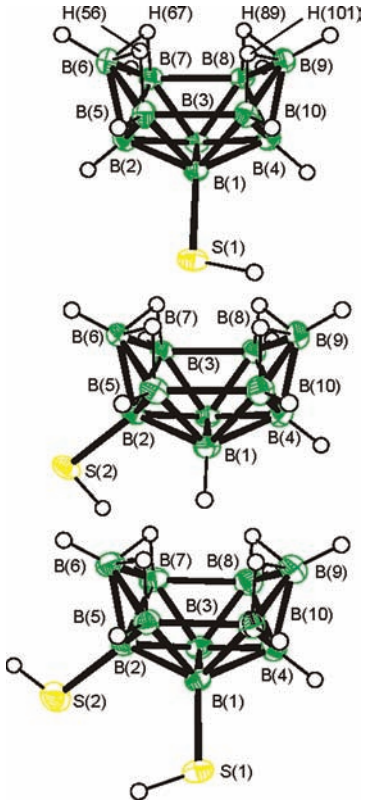

Figure 1. Crystallographically determined molecular structures of [1-(HS)-*nido*-$B_{10}H_{13}$] **1** (top), [2-(HS)-*nido*-$B_{10}H_{13}$] **2** (center), and [1,2-$(HS)_2$-*nido*-$B_{10}H_{12}$] **3** (bottom), with 50% probability ellipsoids for the non-hydrogen atoms. Listings of geometric parameters are given in the Supporting Information.

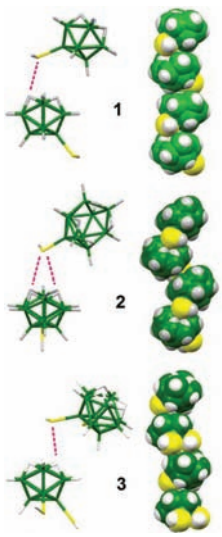

Figure 2. Stick drawings of part of the crystallographic structures of **1**, **2**, and **3** illustrating the S···*μ*-H(BB) hydrogen bond interactions together with space-filling drawings of the resultant stacking of the molecules in which the *c*-axis is perpendicular to the page for **1** and the *b*-axis is perpendicular to the page for **2** and **3**.

1.8039(19) and 1.805(3) Å, which are longer than the equivalent distance in **2** of 1.7856(19) Å.

A point of interest in the crystal structures, and one which relates to the hydrophilicity of the self-assembled monolayers of these compounds discussed later, may be found in the solid-state stacking of compounds **1** to **3** (Figure 2 below) arising from an interaction between the relatively positive bridging hydrogen atoms (compared to the hydridic character of the terminal BH hydrogen atoms) on the open face of the clusters, and the electron density on the sulfur atom of a neighboring cluster. In [2-(HS)-*nido*-$B_{10}H_{13}$] **2**, the sulfur atom is almost equidistant from the four bridging hydrogen atoms, 2.97 to 3.08 Å (Bondi[13] and Pauling[14] van der Waals radii for sulfur 1.80 and 1.85 Å, respectively, hydrogen 1.2 Å). In **1**, the S(1) atom is closer to two of the bridging hydrogen atoms, with measured intermolecular distances S(1) to H(67) and H(89) of 2.98 and 2.95 Å, respectively, compared to the distances to H(56) and H(101) of 3.24 Å each. For **3**, the S(1) atom is also closest to two of the bridging hydrogen atoms, similar to that for **1**, although the distances are longer at 3.02 and 3.14 Å.

dx.doi.org/10.1021/ic202000b | *Inorg. Chem.* 2012, 51, 1685−1694

Dihydrogen S−H···H−B bonds between metallacarborane cage-bound S−H groups and terminal B−H hydrogen atoms have been described previously,[15] but, to our knowledge, an interaction between sulfur and the bridging hydrogen atoms of a borane cluster has not been described before. However, a related interaction between the bridging hydrogen atoms of *nido*-$B_{10}H_{14}$ and π-electron density of the phenyl ring of toluene solvent molecules has been suggested.[16] The presence of an ordered borane-solvent interaction was inferred from the calculation of the molecular tumbling of the solvate pair in toluene-d^8 solution derived from measured NMR data. Similarly, a structurally characterized benzene solvate of $B_{18}H_{22}$ has been reported[17] in which the centroid of the benzene molecule lies close to one of the bridging hydrogen atoms of the *nido*-decaboranyl-structured subclusters at a distance of 2.82 Å. Here, DFT calculations at the B3LYP/6-31+G(d,p) level gave an interaction energy of −1.0 kcal mol^{-1} for the weakly bound solvate pair, $B_{18}H_{22}\cdot C_6H_6$.[17]

This last report also lists a number of short contacts between the bridging hydrogen atoms in boron hydride cluster compounds and aromatic ring centroids obtained from a search of the Cambridge Structural Database (CSD). We have made a further CSD search[18] for other close interactions involving decaborane cluster bridging hydrogen atoms that do not involve aromatic rings. We found a number of contacts between boron-cage terminal hydrogen atoms and bridging hydrogen atoms on adjacent clusters ranging from 2.17 Å, to two bridging H atoms, in [6-(C_6H_5)-*nido*-$B_{10}H_{13}$][19] and in [7,7-$(PMe_2Ph)_2$-*nido*-7-$PtB_{10}H_{11}$-(6′-*nido*-$B_{10}H_{13}$],[20] and also 2.22 Å to a single bridging hydrogen atom in [6,6′-(2,5-norbornyl)-$(B_{10}H_{13})_2$].[21] These contacts were not described in their respective papers but they are significantly shorter than the sum of the van der Waals radii of 2.40 Å and are indicative of a dihydrogen bonding interaction. A further example more relevant to the interaction of the thiol sulfur atom involves intermolecular contacts of a C═O oxygen atom to all four bridging hydrogen atoms of an adjacent cluster and is found in [6-{$CH_3C(O)(CH_2)_4$}-$B_{10}H_{13}$].[22] Here, the oxygen atom lies closer to two of the four bridging hydrogen atoms of a neighboring molecule at a distance of about 2.48 Å, which may be compared to the 2.78 and 2.68 Å distance for the sulfur atom in **1** and **2**, respectively (vdW radii: S 1.80, O 1.52, H 1.20 Å).[13] Similarly, in [6-(CF_3SO_3)-*nido*-$B_{10}H_{13}$] one oxygen atom lies at about 2.54 Å (average of two distances) from the H(67) and H(89) bridging hydrogen atoms.[19]

We carried out further DFT calculations on pairs **1**, **2**, and **3**, respectively, to see if the interaction would remain in the hypothetical gas phase, using, to aid comparison, the same methodology and basis sets used for $B_{18}H_{22}\cdot C_6H_6$. The final orientation of the calculated pair in **2** closely matches that observed in the crystal structure. For example, the angle between the planes defined by the B(5,7,8,10) vertices of the two molecules in the gas phase calculation is 79.9°, which is reasonably close to the 90° angle in the crystal. In **1** there are two similar minima in which the sulfur atom is closest to either the H(67) and H(78) or the H(56) and H(101) pairs of bridging hydrogen atoms, but the lowest minimum is that corresponding to the observed crystal structure, with the angle between the planes defined by the B(5,7,8,10) vertices at 30.2° measured and 27.2° calculated. As mentioned above, the dithiol **3** (Figure 2) adopts a similar orientation to that in **1** with the sulfur atom on B(1) closest to the two H(56), H(101) bridging hydrogen atoms with measured distances of 3.02 and 3.14 Å respectively. The calculated distances of 3.25 and 3.37 Å are somewhat longer, but the calculation does reproduce the difference between the two values of 0.12 Å.

The intermolecular interaction energies for these two-molecule assemblies of these compounds are calculated to be −2.3 for **1**, −3.5 for **2**, and −2.9 kcal mol^{-1} for **3** (summarized in Supporting Information, Table S2). The difference in interaction energies between **2** on one hand, and **1** or **3** on the other hand, reflects the fact that whereas in **1** and **3** the sulfur atom interacts with two bridging hydrogen atoms, in **2** the interaction is with all four. In $B_{18}H_{22}\cdot C_6H_6$ the centroid of the benzene ring is close to only one bridging hydrogen atom of one decaboranyl subcluster.[17] Although it is recognized that the B3LYP functional is not well-suited to the calculation of correlation energies such as in van der Waals attractions and aromatic ring-stacking,[23] the broadly comparable −1.0: −2.3: −3.5: −2.9 kcal mol^{-1} sequence of relative energies very roughly corresponds to the number of bridging hydrogen atoms with which the electron-rich entity interacts, thereby suggesting that the interactions of the open face with the sulfur atom and with the aromatic ring are similar. Clearly, these distances in **1** to **3** are close to the sum of the van der Waals radii and, therefore, the nature of the interaction is uncertain, thus raising the question as to whether the supramolecular structure is due to intermolecular forces such as weak hydrogen-bonding,[24] or to weaker dispersion forces. Though the distances are long it may be noted that, for a hydrogen-bonding interaction, the criterion that the H···Acceptor distance must be substantially shorter than the sum of the van der Waals radii has been questioned, with the suggestion that H···A distances of up to 3.2 Å may be acceptable.[25] Additionally, bifurcated (in **1** and **3**) or tetrafurcated (in **2**) hydrogen bonds would reasonably be expected to show higher donor−acceptor separations. That the observed structures result from electrostatic interactions greater than dispersion forces is supported by the calculations we have carried out for the interaction of H_2S or C_6H_6 with $B_{10}H_{14}$, which afford very similar values of −1.7 and −2.0 kcal mol^{-1} respectively (Supporting Information, Table S3, Figure S1). As mentioned earlier, the aromatic-$B_{10}H_{14}$ interaction is sufficiently strong to manifest in solution.[16]

Platinaundecaborane derivatives of compounds **1** and **2** were prepared in good yield by the simple addition of dichloromethane solutions of $[PtMe_2(PMe_2Ph)_2]$ to dichloromethane solutions of **1** or **2** to afford [1-(HS)-7,7-$(PMe_2Ph)_2$-*nido*-7-$PtB_{10}H_{11}$] **4** (87%) or [4-(HS)-7,7-$(PMe_2Ph)_2$-*nido*-7-$PtB_{10}H_{11}$] **5** (75%), respectively (eq 1).

$$[B_{10}H_{13}(SH)] + [PtMe_2(PMe_2Ph)_2] \rightarrow [(PMe_2Ph)_2PtB_{10}H_{11}(SH)] + 2CH_4\uparrow \quad (1)$$

Insufficient quantities of **3** were available for an analogous reaction to be carried out. Table 2 lists the measured ^{11}B, ^1H, and ^{31}P NMR data for the compounds, together with DFT-calculated nuclear shielding values carried out to aid assignments to the boron cluster vertices. Molecular structures were obtained from single-crystal X-ray diffraction analyses, and drawings are shown in Figure 3. No cluster isomerization, sometimes seen in *nido*-decaboranyl cluster reactions,[26] was observed here, which suggests that the reaction may proceed, in gross terms, by a simple addition of the {$(PMe_2Ph)_2Pt$} moiety across the *nido*-decaboranyl B(6)−B(7) and B(8)−B(9) vectors. Geometrical parameters are generally similar to those for unsubstituted [7,7-$(PMe_2Ph)_2$-*nido*-7-$PtB_{10}H_{12}$].[27] The introduction of

dx.doi.org/10.1021/ic202000b | Inorg. Chem. 2012, 51, 1685−1694

Table 2. Measured ^{11}B, ^{31}P, and ^{1}H NMR Chemical Shift Data for Compounds [1-(HS)-7,7-$(PMe_2Ph)_2$-*nido*-7-$PtB_{10}H_{11}$] 4, [4-(HS)-7,7-$(PMe_2Ph)_2$-*nido*-7-$PtB_{10}H_{11}$] 5[a]

4			5		
assignment	$\delta(^{11}B)$	$\delta(^{1}H)$	assignment	$\delta(^{11}B)$	δ (^{1}H)
5	+18.1[+24.4]	+4.05	5	+17.3[+23.4]	+3.94
2,3	+14.2{194}[b] [+19.3]	+3.62{27}[b]	2	+15.1[+20.6]	+3.56
1	+10.9[+17.0]	*c*	3	+12.9[+18.9]	+3.45
8, 11	+6.1[+10.3]	+2.93	8	+9.5[+14.7]	+3.52
9, 10	−1.0[+3.6]	+2.64	11	+7.6[+13.0]	+2.90
4,6	−25.8[−26.3]	+1.34{37}[b]	1	+3.2[+6.6]	+2.82
			10, 9	−2.9[+2.7,−0.4]	+2.62, +2.59
			4	−17.7[−12.6]	*c*
			6	−26.0[−24.9]	+1.44
S-*H*		+0.73[+1.22][d]	S-*H*		+0.04[+0.47][e]
μ-(8,9; 101)		−2.05[−1.71]	μ-(8,9)		−1.34[−1.01]
			μ-(101)		−2.01[−1.63]
PCH_3[f]		+1.85{12, 25}			+1.92 {9.8, 25} +1.35 {9.6, 24}
		+1.64{10, 26}			+1.72 {9.8, 24} +1.67 {9.7, 21}
$^{31}P\{J(^{31}P-^{31}P)\}$		−40 °C in $CDCl_3$			−50 °C in CD_2Cl_2
		+0.55{2663}			+0.74{2533}
					+0.72{2540}

[a]In CD_2Cl_2 solution at 300 K with B3LYP/6-31G* DFT-calculated shielding data in [square brackets]. [b]$J(^{195}Pt-^{1}H)$ /Hz. [c]Thiol substituent position. [d]Sharpens on $^{1}H-\{^{11}B$ selective} irradiation at $\delta(^{11}B)$ −10.9 ppm. [e]Sharpens on $^{1}H-\{^{11}B$ selective} irradiation at $\delta(^{11}B)$ −17.7 ppm. [f]$N(^{31}P-^{1}H)$ and $^{3}J(^{195}Pt-^{1}H)$ /Hz in {curly brackets}.

the metal fragment slightly lengthens the B−S distances, to 1.894(4) in **4** and 1.894(5) Å in **5** (Figure 3), compared to those in the decaborane thiol precursors which range from 1.8800(13) in **1** to 1.8744(18) Å in **3**. In the DFT-calculated minimized geometries, the S−H group points toward the base of the cluster, similar to that seen in the nonmetalated decaboranyl precursor. Another slightly higher local minimum was identified at a 180° rotation of the SH group around the B−S vector.

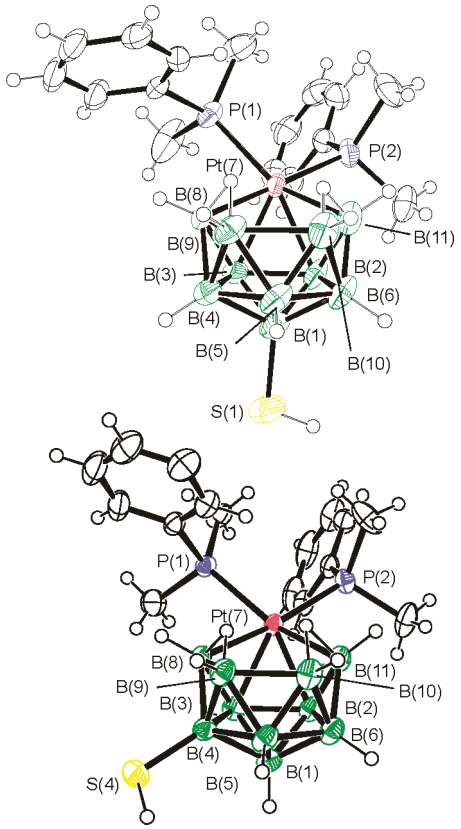

Figure 3. Crystallographically determined molecular structures of [1-(HS)-7,7-$(PMe_2Ph)_2$-*nido*-7-$PtB_{10}H_{11}$] **4** (upper) and [4-(HS)-7,7-$(PMe_2Ph)_2$-*nido*-7-$PtB_{10}H_{11}$] **5** (lower) with 50% probability ellipsoids for the non-hydrogen atoms. A CH_2Cl_2 solvent molecule in **5** is not shown. Listings of geometric parameters are given in the Supporting Information.

X-Ray Photoelectron Spectroscopic (XPS) and Computational Analysis. We have investigated the electronic character of the boron atoms B(1) and B(2) in the decaborane skeletons of the two positional isomers [1-(HS)-$B_{10}H_{13}$] **1** and [2-(HS)-$B_{10}H_{13}$] **2** using the complementary methods of NMR spectroscopy, XPS, and calculated atomic charges. As stated above, a good correlation was found between the GIAO-calculated nuclear shieldings and the measured NMR chemical shifts for the cluster compounds, including the thiol protons. With regard to the correlation between charge distribution and chemical shift, the relative deshielding of the proton in S−H(1) in [1-(HS)-$B_{10}H_{13}$] **1** at $\delta(^{1}H)$ +1.49 ppm compared to S−H(2) in [2-(HS)-$B_{10}H_{13}$] **2** at +0.12 ppm can be taken to suggest that the electron-withdrawing effect of the B(1) vertex is greater than for B(2); here it may be noted that the calculated charge on B(1) of −0.17*e* in [1-(HS)-$B_{10}H_{13}$] is lower than for B(2) in [2-(HS)-$B_{10}H_{13}$] at −0.22*e* (Natural Population Analysis, Scheme 2, see Supporting Information,

Scheme 2. Calculated Atomic Charges on the Boron Atom Vertices B(1) in [1-(HS)-$B_{10}H_{13}$] and B(2) in [2-(HS)-$B_{10}H_{13}$], Together with the Measured Thiol Proton NMR Chemical Shifts

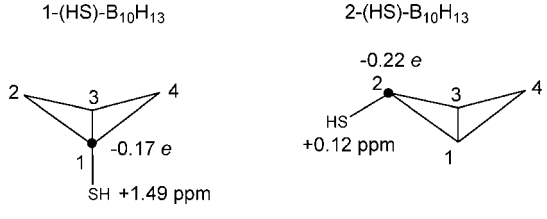

dx.doi.org/10.1021/ic202000b | *Inorg. Chem.* 2012, 51, 1685−1694

Table S1 for a complete listing of the calculated atomic charges). This is in agreement with the trend in *nido*-$B_{10}H_{14}$ itself.[28] The electron-withdrawing effect of the sulfur atom S(1) would therefore be greater than for S(2) as it is attached to a less negatively charged boron vertex. Consistent with this, the calculated charge on S(1) of −0.02*e* is less than for S(2), at −0.08*e*.

Using XPS, we have experimentally investigated compounds **1** and **2** immobilized as two-dimensional self-assembled thiolate monolayers (**1**-SAM and **2**-SAM respectively) on gold and silver flat surfaces. Of particular value in this analysis, with regard to our previous discussion, are the binding-energy (BE) values of the S 2p electrons as shown in Table 3. 1-SAM shows

Table 3. XPS Data: BE of S $2p_{3/2}$ Electrons in eV[a] for Silver and Gold Mounted Decaborane Thiol Compounds 1 to 3

	Ag	Au	stoichiometry on Ag
1-HS-$B_{10}H_{13}$ **1**-SAM	161.6 (2.3)	161.7 (1.8)	$B_{10}S_{1.2}$
2-HS-$B_{10}H_{13}$ **2**-SAM	162.0 (2.2)	162.0 (1.9)	$B_{10}S_{1.2}$
1,2-$(HS)_2$-$B_{10}H_{12}$ **3**-SAM	161.7 (2.2)		$B_{10}S_{2.0}$

[a]With full width at half maximum (FWHM) in parentheses.

a lower binding energy value of 161.6 eV for the S 2p electrons in comparison to **2**-SAM at 162.0 eV, suggesting that the sulfur atom bears a higher negative charge. This difference is analogous to that observed between the two isomers of *ortho*-carborane, 1,2-$(HS)_2$-1,2-$C_2B_{10}H_{10}$ and 9,12-$(HS)_2$-1,2-$C_2B_{10}H_{10}$, self-assembled on a gold surface. Here, a variation of 0.5 eV in the energies of S 2p electrons reflects the different positions of the thiol substituents on the carborane cluster.[4,29] The measured difference in the BE values for **1**-SAM and **2**-SAM are in agreement with the relatively more shielded nature of the thiol proton in the free molecule, [2-(HS)-$B_{10}H_{13}$] **2**, as evident from the ^{1}H NMR spectra. For the dithiol compound, [1,2-$(HS)_2$-$B_{10}H_{12}$] **3**, the case is less clear as the binding energies of the two different sulfur atoms cannot be distinguished at the level of resolution of the XPS spectrometer, and they show as a single peak at 161.7 eV, clearly close to the values for the two monothiol species **1** and **2**.

The measurement of wetting angles is a fundamental part of the macroscopic characterization of modified surfaces and provides information about the hydrophilic or hydrophobic character of the surfaces. Silver surfaces modified with derivatives **1**, **2**, and **3** exhibit wetting angles of 57.7° for **1**-SAM and 55.3° for both **2**- and **3**-SAM. The measured values are effectively the same and demonstrate that their surfaces are relatively hydrophilic compared to a silver surface modified with a thiolated carborane such as [1,2-$(HS)_2$-*closo*-1,2-$C_2B_{10}H_{10}$][6] in which the terminal BH vertices are orientated upward and thus making the surface relatively hydrophobic with a wetting angle of 76°. Conversely, the hydrophilic characters of **1**-SAM, **2**-SAM, and **3**-SAM can be rationalized as resulting from the orientation of the open face of the *nido*-decaboranyl clusters on the surface with their open faces and their associated acidic bridging hydrogen atoms[30] facing upward (illustrated in Scheme 3). The hydrophilic nature also

Scheme 3. Schematic Representation of the Decaborane Thiol Self-Assembled Monolayer

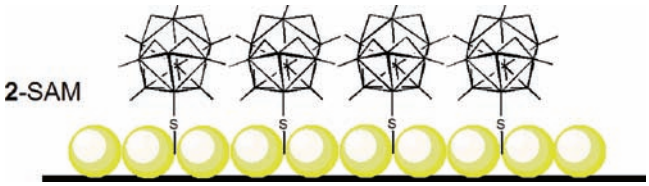

nicely ties in with the acid−base interaction between the bridging hydrogen atoms and the sulfur atom noted in the crystal packing of the molecules discussed above. This, therefore, tends to confirm that the packing of the molecules on the surface is as expected from their rigid molecular architectures: the thiol groups on the basal vertices of the ten-vertex cluster compounds will attach to the metal surfaces so that the open faces of the clusters are distal from the metal surface. The surface density of the SAMs were not explicitly measured, but XPS analysis displayed comparable boron concentrations for all the samples and the surface coverage was sufficient to easily follow the further reactivity of the immobilized molecules.

The volatile character of **1**, **2**, and **3** makes XPS characterization in their bulk form difficult, and we have therefore extended our studies to bulk samples of the two nonvolatile monometallaborane derivatives **4** and **5**, their nonvolatility thus allowing their analysis using XPS. XPS elemental analyses for these metallaborane thiol species are summarized in Table 4. A good agreement between the measured and the nominal stoichiometry was observed. For the sulfur moieties in these compounds, in contrast to **1**-SAM and **2**-SAM where the difference in the nature of their sulfur atom is apparent, there is no significant variation in the BE values of the S 2p electrons

Table 4. Core Level Binding Energies in eV[a] and Elemental Concentrations Determined from XPS Analysis for [1-(HS)-7,7-$(PMe_2Ph)_2$-*nido*-7-$PtB_{10}H_{11}$] 4, [4-(HS)-7,7-$(PMe_2Ph)_2$-*nido*-7-$PtB_{10}H_{11}$] 5, and [7,7-$(PMe_2Ph)_2$-*nido*-7-$PtB_{10}H_{12}$] 6, 4-SAM-a Prepared from Compound 4 and 4-SAM-b Prepared from 1-SAM

	Pt $4f_{7/2}$	P $2p_{3/2}$	S $2p_{3/2}$	B 1s	stoichiometry[b]
4	73.2 (1.3)	131.5 (1.1)	162.6 (1.2)	188.5(1.8)	$[Pt_{1.00}P_{2.05}C_{14.2}S_{1.03}B_{11.0}]$[d]
5	73.2 (2.0)	131.2 (2.1)	162.5 (2.4)	188.7 (2.2)	$[Pt_{1.00}P_{2.00}C_{16.7}S_{1.0}B_{9.8}]$[d]
6	73.2 (1.2)	131.4 (1.1)		188.4(1.7)	$[Pt_{1.00}P_{2.06}C_{15.9}B_{10.7}]$[e]
4-SAM-**a**	73.1 (1.9)	131.5 (1.8)	162.3[66][c] 168.7 [33]	188.6(2.4)	$[Pt_{1.00}P_{1.0}C_{21.4}S_{1.00}B_{10.0}]$[d]
4-SAM-**b**	73.2(1.8)	131.6(1.3)	162.0[78][c] 164.4[22]	188.6(1.8)	$[Pt_{1.00}P_{0.80}C_{18.5}S_{1.00}B_{7.60}]$[d]

[a]With full width at half maximum (FWHM) in parentheses. [b]Because of overlap of P 2s and B 1s lines, the determination of the concentration of boron is less accurate than that of the other elements. [c]Values in square brackets are populations of different chemical states of sulfur. [d]Nominal values for $[(PMe_2Ph)_2PtB_{10}H_{11}(SH)]$: $Pt_1P_2C_{16}S_1B_{10}$. [e]Nominal values for $[(PMe_2Ph)_2PtB_{10}H_{12}]$: $Pt_1P_2C_{16}B_{10}$.

dx.doi.org/10.1021/ic202000b | *Inorg. Chem.* 2012, 51, 1685−1694

between the metallaborane derivatives **4** and **5**. The ^{1}H NMR chemical shifts of their respective SH groups show a narrowing from a shielding difference $\Delta\delta(^{1}H)$ of 1.37 ppm in **1** versus **2** to only 0.69 ppm in **4** versus **5**. This suggests that the insertion of a platinum atom into the cluster influences the character of the SH groups. This is of importance as it bears on one of our general aims in this area: the investigation of the effect of substituents attached to the boron framework on the properties of the metal centers in bimetallic $[(PMe_2Ph)_4M_2B_{10}H_{10}]$ cluster compounds and thence the strengthening or weakening of the binding of small molecules on the metal−metal vector.[9] This result might suggest that there is a mutual interaction that is worthy of further investigation. However, the addition of a SH substituent to the cluster shows no measurable effect on the binding energy values of the Pt $4f_{7/2}$ electrons, which are 73.2 eV, both in thiol-containing $[1\text{-}(HS)\text{-}7,7\text{-}(PMe_2Ph)_2\text{-}nido\text{-}7\text{-}PtB_{10}H_{11}]$ **4** and in the nonthiol compound $[7,7\text{-}(PMe_2Ph)_2\text{-}nido\text{-}7\text{-}PtB_{10}H_{12}]$ **6**.

This difference between the metalated and the nonmetalated species may exhibit better in the binding energies of the S 2p electrons. For the nonmetalated compounds **1**, **2**, and **3** on gold and silver surfaces, these range from 161.6 to 162.0 eV and are typical of thiolate moieties.[4] The values for the S 2p electrons in both platinum derivatives **4** and **5** are shifted higher, to 162.6 eV, as may be expected for a more positive sulfur atom in a neutral thiol group although this value is still lower than those commonly found for SH groups in organic compounds, for example, 163.3 eV for thiophenol,[31] or 163.6 and 163.8 eV, respectively, for the free thiol groups in $[1,12\text{-}(HS)_2\text{-}1,12\text{-}closo\text{-}C_2B_{10}H_{10}]$ or 1,5-pentanedithiol assembled on a gold surface.[29,32]

Preliminary investigations on monolayers of the metallaboranes **4** and **5** have indicated that the interaction with the surface is less straightforward than for their simple borane precursors, giving results in the XP spectra which do not conform precisely to the expected stoichiometry. We have directed our attention to the $[1\text{-}(HS)\text{-}B_{10}H_{13}]$ isomer and its metallaborane derivative following two different synthetic strategies for the formation of the self-assembled monolayers as illustrated in Scheme 4. Immersion of a gold substrate in a solution

Scheme 4. Reaction Scheme for the Preparation of 4-SAM-a and 4-SAM-b, Showing Also the Binding Energies of the Sulfur 2p Electrons

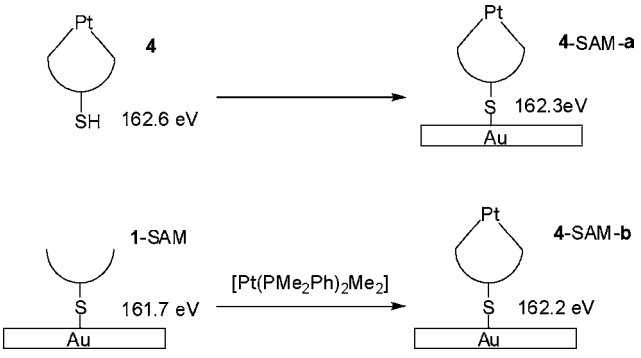

of $[1\text{-}(HS)\text{-}7,7\text{-}(PMe_2Ph)_2\text{-}nido\text{-}7\text{-}PtB_{10}H_{11}]$ **4** produced **4**-SAM-**a**, for which XPS analysis showed a stoichiometry of $Pt_{1.00}P_{0.93}C_{19.4}S_{1.00}B_{9.60}$. The carbon 1s XP spectrum is influenced by the presence of hydrocarbon impurities that may be originating, for example, from the solvents used for SAM preparation or from the laboratory atmosphere. The spectrum consists of three components with binding energies 284.8, 286.0, and 288.9 eV. The predominant component (ca. 70%) is characteristic of C−C and C−H bonds commonly found in hydrocarbons. The second component (ca. 20%) can be attributed to C−OH moieties, and the third component (ca. 10%) is attributable to O−C═O functionalities. Overall (Table 4), the main difference, when compared to the bulk compound, is the apparent loss of one phosphorus atom or phosphine ligand.

An alternative synthetic strategy for a SAM of the platinated compound **4** is the immersion of nonplatinated **1**-SAM in a solution of $[PtMe_2(PMe_2Ph)_2]$ in dichloromethane (Scheme 4, lower diagrams). The product resulting from this second synthetic strategy exhibits roughly similar stoichiometry to **4**-SAM-**a**, namely, $Pt_{1.00}P_{0.80}C_{18.5}S_{1.00}B_{7.60}$ (**4**-SAM-**b**) (Table 4). Again there is an apparent loss of one phosphorus atom or phosphine ligand. These results were reproduced in three independent trials for **4**-SAM-**a** and **4**-SAM-**b**, and they remain unexplained. The loss of phosphine ligand from the metal during the insertion of a $\{(PMe_2Ph)_2Pt\}$ moiety into a borane clusters is highly unusual. A rare example is seen in the original isolation of $[(PMe_2Ph)_4Pt_2B_{10}H_{10}]$ in which small amounts of $[Cl(PMe_2Ph)_3Pt_2B_{10}H_9(PMe_2Ph)]$ was isolated and where a phosphine ligand migrated from a platinum center to the cluster, with concomitant replacement by chlorine.[33]

The S 2p spectra of samples **4**-SAM-**a** and **4**-SAM-**b**, exhibit, respectively, two and one additional minor components, both of which may be assigned to oxidized sulfur species, and this suggests that metallaborane samples, chemisorbed on the substrate surface via an SH group, are more sensitive toward oxidation under ambient conditions than the bulk compound **4**; future work in this system will require more stringent anaerobic conditions.

CONCLUSIONS

This study introduces, for the first time, the potential for open-faced borane clusters to act as a new class of reactive building blocks for the construction of novel and functional self-assembled molecular monolayers. Three decaborane thiol cluster compounds are characterized by the complementary techniques of single-crystal X-ray diffraction, multielement NMR spectroscopy, DFT structure and GIAO nuclear-shielding calculations, and by computational charge-distribution analysis. The X-ray structures of **1** to **3** reveal that interaction between the hydridic BHB hydrogen atoms of the 10-vertex *nido*-clusters and the sulfur atom of the thiol groups leads to the formation of bi- and tetra-furcated hydrogen bonds that direct the packing of the SH-substituted decaboranes in the crystal structures. The decaborane thiols are used to form self-assembled monolayers on silver and gold substrates anchored by the sulfur atom, and wetting-angle goniometry shows a lower hydrophobicity compared to monolayers of 12-vertex carboranes because of the presence of the four hydridic BHB hydrogen atoms on the surface. The orientation of the clusters with their open faces pointing upward from the surface is as expected from the geometrical disposition of the open face relative to the position of the sulfur substituent.

The presence of the reactive, hydridic, bridging hydrogen atoms on the surface provides sites for further chemistry similar to that of the bulk compounds. This is shown by the reaction of a SAM preprepared from $[1\text{-}(HS)\text{-}B_{10}H_{13}]$ **1** with a solution of $[PtMe_2(PMe_2Ph)_2]$. The resultant SAM, **4**-SAM-**b**, exhibits similar stoichiometry to that of a SAM, **4**-SAM-**a**, prepared directly from $[1\text{-}(HS)\text{-}7,7\text{-}(PMe_2Ph)_2\text{-}nido\text{-}7\text{-}PtB_{10}H_{11}]$ **4**.

dx.doi.org/10.1021/ic202000b | Inorg. Chem. 2012, 51, 1685−1694

In summary, we have demonstrated that reactive boron hydride clusters can assemble on metal surfaces, and, by undergoing a cluster insertion of a metal moiety, we demonstrate that they ostensibly retain their original reactivity. This is an unprecedented observation and may, in principle, be extended to a range of other boron hydride clusters. In particular, this work represents a step toward our goal of the assembly of chemically active bimetallaborane moieties[9b,34] on metal surfaces.

EXPERIMENTAL SECTION

General Procedures. Dried, deoxygenated solvents were stored over a suitable drying agent in evacuated flasks sealed with a high-vacuum Teflon stopcock. Reactions were carried out using standard Schlenk-line vacuum techniques although subsequent isolations were carried out in air. NMR samples were prepared by condensing deuterated solvents on to the sample in 5 mm o.d. NMR tubes equipped with a Teflon vacuum tap. NMR spectroscopy was performed at about 7.1 T (field corresponding to nominal 300 MHz ^{1}H frequency) using commercially available instrumentation and using standard techniques and procedures.[35] The nonthiolated platinaborane [7,7-$(PMe_2Ph)_2$-*nido*-7-$PtB_{10}H_{12}$] **6** and [$PtMe_2(PMe_2Ph)_2$] were prepared as described previously.[10,36]

Compound Syntheses. *Synthesis of [1-(HS)-nido-$B_{10}H_{13}$] **1**, [2-(HS)-nido-$B_{10}H_{13}$] **2**, and [1,2-$(HS)_2$-nido-$B_{10}H_{12}$] **3**.* The thiolated decaboranyl compounds were prepared by a modified literature method[8] from $B_{10}H_{14}$ (2.48 g, 20 mmol), $AlCl_3$ (3.7 g, 28 mmol), and elemental sulfur (1.29 g, 40 mmol). Following the original procedure,[8] we found sublimation of the starting materials from the reaction mixture to be a problem, and the claimed yield of 50% of a mixture of isomers **1** and **2** was difficult to reproduce. We used an evacuated sealed glass tube heated at about 120 °C in an oil bath overnight. (Warning: some pressure does build up in the sealed tube and appropriate safety precautions should be taken). Following the extraction by hexane of the resultant solid (3.17 g) to remove remaining $B_{10}H_{14}$, ice−water was added to the solid and then it was acidified with 10% HCl. The ensuing aqueous solution was extracted with hexane and the hexane removed on a rotary evaporator, and the resulting solid sublimed in vacuo at 80 °C. The sublimate was dissolved in hot cyclohexane and left in a refrigerator overnight affording a white solid. After filtration and washing with cold pentane, the solid was found to be pure by NMR spectroscopy, and was identified as [2-(HS)-*nido*-$B_{10}H_{13}$] **2** (0.105 g). Subsequent crystallizations and recrystallizations of the solids from the cyclohexane filtrate afforded a combined yield of 0.26 g, 8% of **2** together with a small amount, 3.3 mg, of [1,2-$(HS)_2$-*nido*-$B_{10}H_{12}$] **3**. The cyclohexane residues contained smaller quantities of [1-(HS)-*nido*-$B_{10}H_{13}$] **1** and were subjected to column chromatography eluted with hexane and then 2:1 benzene/hexane as described in ref 8, affording a pure sample of **1** (85 mg, 3%). The yields were lower than those originally claimed but were sufficient for the purposes of the work described herein. Further thiolation of the monothiol compounds to give the dithiol **3** would be a route to larger quantities, but attempts to maximize its yield have not yet been made.

*Synthesis of [1-(HS)-7,7-$(PMe_2Ph)_2$-nido-$PtB_{10}H_{11}$] **4** and [4-(HS)-7,7-$(PMe_2Ph)_2$-nido-$PtB_{10}H_{11}$] **5**.* A magnetic stir bar and freshly prepared [1-(HS)-$B_{10}H_{13}$] **1** (87.4 mg, 0.566 mmol) were placed in a 100 mL, 2-neck round-bottomed flask, the flask was evacuated, and CH_2Cl_2 (ca. 10 mL) was condensed into the flask. Nitrogen was allowed into the flask to restore ambient pressure. The mixture was stirred to dissolve. Similarly, CH_2Cl_2 (ca. 10 mL) was also condensed into a flask containing [$PtMe_2(PMe_2Ph)_2$] (0.284 g, 0.566 mmol). The flask was agitated to dissolve the material giving a clear solution, and the resulting solution was then injected via syringe into the first flask through a 0.2 μm syringe filter. A further 10 mL of CH_2Cl_2 was condensed into the second flask and added to the first flask to ensure complete transfer of the metal starting material. After about 5 min of stirring, the reaction mixture was left for about 2 h during which time a clear yellow solution formed. NMR spectroscopy of a small aliquot showed a single product. A large volume of *n*-pentane, about 50 mL, was then condensed on top of the CH_2Cl_2 layer, and the mixture was left for about 2 days. The large needle-shaped crystals thus formed were filtered off in air, washed with pentane, and identified as [1-(HS)-7,7-$(PMe_2Ph)_2$-*nido*-7-$PtB_{10}H_{11}$] **4** (0.308 g, 0.492 mmol, 87%). Analysis: calculated: C 30.81, H 5.5; found: C 30.93, H 5.7%. Similarly to the above procedure, [2-(HS)-$B_{10}H_{13}$] afforded a 75% yield of [4-(HS)-7,7-$(PMe_2Ph)_2$-*nido*-7-$PtB_{10}H_{11}$] **5**, although, in this case, the product consisted of a microcrystalline powder. Single-crystals of **4** and **5** suitable for X-ray diffraction analysis were obtained by pentane diffusion into CH_2Cl_2 solutions of the compounds.

SAM Preparation. *Nido*-decaboranyl thiolate SAMs were prepared by dissolving a quantity (**1**, 7.6 mg; **2**, 8.8 mg; **3**, 3.0 mg) of the respective compound in 2 mL of CH_2Cl_2 (freshly distilled after standing over K_2CO_3) and then passing the solution through a syringe filter (0.2 μm, PVDF, Whatman) into a new sample tube. The gold substrate comprised a 200 nm thick gold film deposited on a glass wafer (11 × 11 mm) by evaporation with a Cr interlayer (Arrandee, Germany), and this was annealed with a hydrogen flame immediately prior to use and allowed to cool under an argon atmosphere as described previously.[4] Silver substrates comprised a silver film deposited on a glass wafer by sputtering under conditions described elsewhere.[7] The substrates were immersed in the respective borane thiol solutions of **1** to **3** for 1 h, then removed, and immediately immersed in a beaker of distilled CH_2Cl_2 to wash, followed by rinsing with an excess of CH_2Cl_2 and drying in a stream of Ar. The metallaborane **4**-SAM-**a** was prepared by immersing a gold substrate in a 5 mL of 0.2 μm filtered dichloromethane solution containing 40.8 mg of **4** for 24 h, after which time the cleaning procedure described above was followed. Similarly, **4**-SAM-**b** was obtained by dissolving **1** (20.1 mg) in 5 mL of dichloromethane to prepare the initial SAM as above and then, after washing in dichloromethane, immediately immersing it in a 2 mL dichloromethane solution of [$PtMe_2(PMe_2Ph)_2$] (14.5 mg) for 4 h. Samples were stored in an atmosphere of nitrogen, and analyzed within 1 day of preparation.

Contact-Angle Measurement. Static contact angles of water (Water G Chromasolv, for gradient elution, Ec. No. 231−791−2) were measured on a Contact Angle Measuring System G10 (KRÜSS GmbH, Hamburg, Germany). An approximately 20 μL drop of water was formed at the end of the needle. The needle was lowered until the drop touched the surface and then raised, detaching the drop. Averages of six measurements of stable static drops were made for each surface.

XPS. Two XP spectrometers were used in this study:

(A) Compounds **1**, **2**, and **3**. X-ray photoelectron spectroscopy (XPS) measurements were carried out on a PHI 5600 instrument, using nonmonochromated Mg or Al-*Kα* radiation and operated at 300 W (13 kV × 23 mA). The operating pressure of the XPS analysis chamber was approximately 5×10^{-9} Torr. The spectra were collected at photoemission angles of 45° with respect to the surface normal. Survey scan spectra (0−1100 eV) and higher-resolution narrow spectra were acquired using analyzer pass energies of 190 and 30 eV, respectively. Curve fitting was carried out with CasaXPS software version 2.3.14 using a mixed Gaussian−Lorentzian product function. The Gaussian-to-Lorentzian ratio was kept constant as 70% Gaussian and 30% Lorentzian. Atomic ratios were calculated from XP spectra after subtracting a Shirley-type background.[37] The accuracy of the measured electron energies was roughly ±0.1 eV.

(B) Compounds **4**, **5**, **6**, **4**-SAM-**a**, and **4**-SAM-**b**. The photoelectron spectra of these samples were measured using an ESCA310 (Scienta, Sweden) electron spectrometer equipped with a hemispherical electron analyzer operated in a fixed transmission mode. Monochromatic Al K*α* radiation was used for electron excitation. The spectrometer was calibrated to the Au $4f_{7/2}$ peak at 84.0 eV. A small amount of powder samples of compounds **4**, **5**, or **6** were spread on a clean Mo surface. The spectra were recorded at room temperature. The Pt 4f, C 1s, P 2p, B 1s, P 2s, S 2p photoelectrons were measured. The electron detection angle was 90° with respect to the macroscopic sample surface. The pressure of residual gases in the analyzer chamber during spectra acquisition was 2×10^{-9} mbar. For calibration of the spectra of powder compounds, the C 1s line at 284.8 eV was used. The accuracy of the measured binding energies was ±0.2 eV for powder samples and ±0.1 eV for SAMs. The spectra were curve fitted after subtraction

dx.doi.org/10.1021/ic202000b | *Inorg. Chem.* 2012, 51, 1685−1694

Table 5. Crystallographic Collection and Refinement Data[a]

	1	2	3	4	5
CCDC	815236	815237	815238	815239	815240
formula	$B_{10}H_{14}S$	$B_{10}H_{14}S$	$B_{10}H_{14}S_2$	$C_{16}H_{34}B_{10}P_2PtS$	$C_{16}H_{34}B_{10}P_2PtS.CH_2Cl_2$
Size	0.27 × 0.21 × 0.15	0.28 × 0.15 × 0.12	0.28 × 0.15 × 0.12	0.28 × 0.22 × 0.08	0.18 × 0.13 × 0.08
formula wt.	154.27	154.27	186.33	623.62	623.62
crystal system	orthorhombic	orthorhombic	monoclinic	monoclinic	orthorhombic
space group	$P2_12_12_1$	$P2_12_12_1$	$P2_1/n$	$P2_1/c$	$P2_12_12_1$
a/Å	7.1271(14)	7.14960(10)	7.4989(5)	10.2839(11)	11.761(2)
b/Å	11.684(2)	10.7261(2)	10.7261(2)	18.928(2)	12.061(2)
c/Å	11.880(2)	12.7584(3)	12.1474(8)	13.9112(16)	21.084(4)
β/deg	90	90	92.084(4)	98.931(6)	90
V/Å^3	989.3(3)	978.41(3)	1074.60(12)	2675.1(5)	2990.7(10)
D_{calc}/g·cm^{-3}	1.036	1.047	1.152	1.548	1.574
F_{000}	320	320	384	1216	1384
data/restr/params	2497/0/156	2423/0/156	2774/0/151	6536/0/300	9071/0/327
μ mm^{-1}	0.245	0.248	0.424	5.446	5.055
GoF	0.832	1.082	1.051	1.12	1.082
$R1$ ($I > 2\sigma(I)$)	0.0266	0.0247	0.0380	0.0408	0.0252
$wR2$ (all data)	0.0757	0.0618	0.1055	0.0959	0.0619
$\rho_{max\ and\ min}$/e$^-$ Å^{-3}	0.20 and −0.12	0.26 and −0.13	0.67 and −0.47	3.6 and −1.9	3.4 and −1.5
Flack	−0.03(6)	0.03(6)			0.014(5)

[a]Common factor: T = 150(2) K, Z = 4.

of Shirley background[37] using the Gaussian−Lorentzian line shape and nonlinear least-squares algorithms. Quantification of the elemental concentrations was accomplished by correcting photoelectron peak intensities for their cross sections[38] and analyzer transmission function. In the calculations, a homogeneous composition of the analyzed layer of the samples measured was assumed.

Crystallography. Diffraction data were measured at 150 K on a Bruker X8 Apex diffractometer, with graphite-monochromated Mo-$K\alpha$ radiation (λ = 0.71073 Å) generated by a rotating anode. The structures were solved and refined using standard methods and programs.[39] The program X-Seed[40] was used as an interface to the SHELX programs, and ORTEP-3 was used to prepare the figures.[41] Selected collection and refinement data are listed in Table 5 together with CCDC numbers. Supplementary crystallographic data can be obtained free of charge via http://www.ccdc.cam.ac.uk/conts/retrieving.html, or from the Cambridge Crystallographic Data Centre, 12 Union Road, Cambridge CB2 1EZ, U.K.; fax: (+44) 1223-336-033; or e-mail: deposit@ccdc.cam.ac.uk.

Computational Details. GIAO nuclear shielding calculations were carried out using the Gaussian03 package.[11a] Structures were initially optimized using standard ab initio methods with the STO-3G* basis-sets for B, P, S, and H and with the LANL2DZ basis-set for Pt for **4** and **5**. The final optimizations, including frequency analyses to confirm true minima, were performed using the B3LYP methodology with the 6-31+G(d,p) basis set for compounds **1** to **3** and the 6-31G* and LANL2DZ basis-sets for **4** and **5**.[11] GIAO NMR nuclear shielding predictions were then performed on the optimized geometries. Computed ^{11}B shielding values were related to chemical shifts by comparison with the computed value for B_2H_6 which was taken to be $\delta(^{11}B)$ +16.6 ppm relative to the $F_3B{\cdot}OEt_2$ = 0.0 ppm standard. The metallaborane compounds were modeled using hydrogen atoms rather than methyl and phenyl groups on the phosphine ligands to reduce computation time.

To calculate the charge distribution, the structures of the species were optimized using the Turbomole[42] quantum chemistry package in the resolution of identity-approximate coupled-cluster singles-and-doubles model (RI-CC2)[43] employing the def2-TZVP[44] triple-ζ basis set with polarization functions and the corresponding auxiliary basis set.[45] For the optimized geometry, the orbital-relaxed values of data were extracted, and their natural population analysis in the atomic orbitals basis was carried out.

■ ASSOCIATED CONTENT

Ⓢ Supporting Information

Additional information includes a table of Turbomole CC2 calculated atomic charges for clusters **1**, **2**, and **3**. Tables of the DFT calculated energies and listings of atomic coordinates for compounds **1** to **5**, and $C_6H_6{\cdot}B_{10}H_{14}$ and $H_2S{\cdot}B_{10}H_{14}$ and tables of selected interatomic distances and angles for compounds **1** to **5**, determined by X-ray crystallography are also included. This material is available free of charge via the Internet at http://pubs.acs.org.

■ AUTHOR INFORMATION

Corresponding Author

*E-mail: jbould@gmail.com (J.B.), tbase@iic.cas.cz (T.B.).

■ ACKNOWLEDGMENTS

This work was supported by the Grant Agency of the Czech Republic (Grants P207/11/1577 and P205/10/0348) and by the Grant Agency of the Academy of Sciences of the Czech Republic (Grants KAN400480701, KAN100400702, IAA 400320901, M200320904). J.B. wishes to thank the Spanish Ministry of Science Innovation for sabbatical funding (SAB2009-0191). We thank Colin Kilner for the collection of the single-crystal X-ray diffraction data.

■ REFERENCES

(1) (a) Love, J. C.; Estroff, L. A.; Kriebel, J. K.; Nuzzo, R. G.; Whitesides, G. M. *Chem. Rev.* **2005**, *105*, 1103. (b) Gooding, J. J.; Ciampi, S. *Chem. Soc. Rev.* **2011**, *40*, 2704.

(2) Ulman, A. *Chem. Rev.* **1996**, *96*, 1533.

(3) Hohman, J. N.; Claridge, S. A.; Kim, M.; Weiss, P. S. *Mater. Sci. Eng., R.* **2010**, *70*, 188.

(4) Baše, T.; Bastl, Z.; Plzák, Z.; Grygar, T.; Plešek, J.; Carr, M. J.; Malina, V.; Šubrt, J.; Boháček, J.; Večerníková, E.; Kříž, O. *Langmuir* **2005**, *21*, 7776.

(5) Hohman, J. N.; Zhang, P. P.; Morin, E. I.; Han, P.; Kim, M.; Kurland, A. R.; McClanahan, P. D.; Balema, V. P.; Weiss, P. S. *ACS Nano* **2009**, *3*, 527.

(6) Baše, T.; Bastl, Z.; Hávranek, V.; Lang, K.; Bould, J.; Londesborough, M. G. S.; Macháček, J.; Plešek, J. *Surf. Coat. Technol.* **2010**, *204*, 2639.
(7) Lübben, J. F.; Baše, T.; Rupper, P.; Künniger, T.; Macháček, J.; Guimond, S. *J. Colloid Interface Sci.* **2011**, *354*, 168.
(8) Janoušek, Z.; Plešek, J.; Plzák, Z. *Collect. Czech. Chem. Commun.* **1979**, *44*, 2904.
(9) (a) Bould, J.; Kennedy, J. D. *Chem. Commun.* **2008**, 2447. (b) Bould, J.; Kilner, C. A.; Kennedy, J. D. *Dalton Trans.* **2005**, 1574. (c) Bould, J.; McInnes, Y. M.; Carr, M. J.; Kennedy, J. D. *Chem. Commun.* **2004**, 2380.
(10) Bould, J.; Baše, T.; Londesborough, M. G. S.; Oro, L. A.; Macías, R.; Kennedy, J. D.; Kubat, P.; Fuciman, M.; Polivka, T.; Lang, K. *Inorg. Chem.* **2011**, *50*, 7511.
(11) (a) Frisch, M. J.; Trucks, G. W.; Schlegel, H. B.; Scuseria, G. E.; Robb, M. A.; ; Cheeseman, J. R.; Jr., J. A. M.; Vreven, T.; Kudin, K. N.; Burant, J. C.; J. M..Millam.; Iyengar, S. S.; Tomasi, J.; Barone, V.; Mennucci, B.; ; Cossi, M.; Scalmani, G.; Rega, N.; Petersson, G. A.; Nakatsuji, H.; Hada, M.; Ehara, M.; Toyota, K.; Fukuda, R.; Hasegawa, J.; Ishida, M.; Nakajima, T.; Honda, Y.; Kitao, O.; Nakai, H.; Klene, M.; Li, X.; Knox, J. E.; Hratchian, H. P.; Cross, J. B.; Bakken, V.; Adamo, C.; Jaramillo, J.; ; Gomperts, R.; Stratmann, R. E.; Yazyev, O.; Austin, A. J.; Cammi, R.; ; Pomelli, C.; Ochterski, J.; Ayala, P. Y.; Morokuma, K.; Voth, G. A.; Salvador, P.; Dannenberg, J. J.; Zakrzewski, V. G.; Dapprich, S.; Daniels, A. D.; Strain, M. C.; Farkas, O.; Malick, D. K.; Rabuck, A. D.; Raghavachari, K.; Foresman, J. B.; Ortiz, J. V.; Cui, Q.; Baboul, A. G.; Clifford, S.; Cioslowski, J.; Stefanov, B. B.; Liu, G.; Liashenko, A.; Piskorz, P.; ; Komaromi, I.; Martin, R. L.; Fox, D. J.; Keith, T.; Al-Laham, M. A.; Peng, C. Y.; Nanayakkara, A.; Challacombe, M.; Gill, P. M. W.; Johnson, B. G.; Chen, W.; Wong, M. W.; Gonzalez, C.; Pople, J. A. In *Gaussian 03*, Rev. C.02; Gaussian, Inc: Wallingford, CT, 2004. (b) Becke, A. D. *J. Chem. Phys.* **1993**, *98*, 5648. (c) Lee, C.; Yang, W.; Parr, R. G. *Phys. Rev. B* **1988**, *37*, 785. (d) Hehre, W. J.; Ditchfield, R.; Pople, J. A. *J. Chem. Phys.* **1972**, *56*, 2257. (e) Hay, P. J.; Wadt, W. R. *J. Chem. Phys.* **1985**, *82*, 299.
(12) Kasper, J. S.; Lucht, C. M.; Harker, D. *Acta Crystallogr.* **1950**, *3*, 436.
(13) Bondi, A. *J. Phys. Chem.* **1964**, *68*, 441.
(14) Pauling, L. *The Nature of the Chemical Bond*, 2nd ed.; Cornell University Press: Ithaca, NY, 1948.
(15) Planas, J. G.; Viñas, C.; Teixidor, F.; Comas-Vives, A.; Ujaque, G.; Lledós, A.; Light, M. E.; Hursthouse, M. B. *J. Am. Chem. Soc.* **2005**, *127*, 15976.
(16) Gibb, T. C.; Kennedy, J. D. *J. Chem. Soc., Faraday Trans. II* **1982**, *78*, 525.
(17) Hamilton, E. J. M.; Kultyshev, R. G.; Du, B.; Meyers, E. A.; Liu, S.; Hadad, C. M.; Shore, S. G. *Chem.—Eur. J.* **2006**, *12*, 2571.
(18) Fletcher, D. A.; McMeeking, R. F.; Parkin, D. *J. Chem. Inf. Comput. Sci.* **1996**, *36*, 746.
(19) Hawthorne, M. F.; Mavunkal, I. J.; Knobler, C. B. *J. Am. Chem. Soc.* **1992**, *114*, 4427.
(20) Shea, S. L.; Bould, J.; Londesborough, M. G. S.; Perera, S. D.; Franken, A.; Ormsby, D. L.; Jelinek, T.; Štíbr, B.; Holub, J.; Kilner, C. A.; Thornton-Pett, M.; Kennedy, J. D. *Pure. Appl. Chem.* **2003**, *75*, 1239.
(21) Wei, X.; Carroll, P. J.; Sneddon, L. G. *Chem. Mater.* **2006**, *18*, 1113.
(22) Kusari, U.; Carroll, P. J.; Sneddon, L. G. *Inorg. Chem.* **2008**, *47*, 9203.
(23) Zhao, Y.; Truhlar, D. G. *Acc. Chem. Res.* **2008**, *41*, 157.
(24) Marcus, S. H.; Miller, S. I. *J. Am. Chem. Soc.* **1966**, *88*, 3719.
(25) Steiner, T. *Angew. Chem., Int. Ed.* **2002**, *41*, 48.
(26) Bould, J.; Dörfler, U.; Thornton-Pett, M.; Kennedy, J. D. *Inorg. Chem. Commun.* **2001**, *4*, 544.
(27) Boocock, S. K.; Greenwood, N. N.; Kennedy, J. D.; McDonald, W. S.; Staves, J. *J. Chem. Soc., Dalton Trans.* **1981**, 2573.
(28) Laws, E. A.; Lipscomb, W. N.; Stevens, R. M. *J. Am. Chem. Soc.* **1972**, *94*, 4467.
(29) Baše, T.; Bastl, Z.; Šlouf, M.; Klementová, M.; Šubrt, J.; Vetushka, A.; Ledinski, M.; Fejfar, A.; Macháček, J.; Carr, M. J.; Londesborough, M. G. S. *J. Phys. Chem. C* **2008**, *112*, 14446.
(30) (a) Guter, G. A.; Schaeffer, G. W. *J. Am. Chem. Soc.* **1956**, *78*, 3546. (b) Stanko, V. I.; Chapovskii, Y. A.; Brattsev, V. A.; Zakharkin, L. I. *Russ. Chem. Rev.* **1965**, *34*, 424.
(31) Barriet, D.; Yam, C. M.; Shmakova, O. E.; Jamison, A. C.; Lee, T. R. *Langmuir* **2007**, *23*, 8866.
(32) Deng, W.; Yang, L.; Fujita, D.; Nejoh, H.; Bai, C. *Appl. Phys. A: Mater. Sci. Process* **2000**, *71*, 639.
(33) Cheek, Y. M.; Kennedy, J. D.; Thornton-Pett, M. *Inorg. Chim. Acta* **1985**, *99*, L43.
(34) Bould, J.; Baše, T.; Londesborough, M. G. S.; Oro, L. A.; Macías, R.; Kennedy, J. D.; Kubát, P.; Fuciman, M.; Polívka, T.; Lang, K. *Inorg. Chem.* **2011**, *50* (16), 7511.
(35) (a) Heřmánek, S. *Chem. Rev.* **1992**, *92*, 325. (b) Kennedy, J. D. In *Multinuclear NMR*; Mason, J., Ed.; Plenum: New York, 1987.
(36) Kaur, P.; Brownless, A.; Perera, S. D.; Cooke, P. A.; Jelínek, T.; Kennedy, J. D.; Štíbr, B.; Thornton-Pett, M. *J. Organomet. Chem.* **1998**, *557*, 181.
(37) Shirley, D. A. *Phys. Rev. B* **1972**, *5*, 4709.
(38) Scofield, J. H. *J. Electron Spectrosc. Relat. Phenom.* **1976**, *8*, 129.
(39) (a) Sheldrick, G. M. *SHELXL97, Program for the refinement of crystal structures*; Bruker AXS: Madison, WI, 1997. (b) Sheldrick, G. *Acta Crystallogr., Sect. A* **2008**, *64*, 112.
(40) Barbour, L. J. *J. Supramol. Chem.* **2001**, *1*, 189.
(41) Farrugia, L. J. *J. Appl. Crystallogr.* **1997**, *30*, 565.
(42) (a) *TURBOMOLE* V6.2 22 2010; University of Karlsruhe and Forschungszentrum Karlsruhe GmbH: Karlsruhe, Germany, 1989–2007. (b) Ahlrichs, R.; Bär, M.; Häser, M.; Horn, H.; Kölmel, C. *Chem. Phys. Lett.* **1989**, *162*, 165.
(43) (a) Christof, H.; Florian, W. *J. Chem. Phys.* **2000**, *113*, 5154. (b) Christiansen, O.; Koch, H.; Jørgensen, P. *Chem. Phys. Lett.* **1995**, *243*, 409. (c) Hättig, C.; Hellweg, A.; Köhn, A. *Phys. Chem. Chem. Phys.* **2006**, *8*, 1159.
(44) Weigend, R. A. *Phys. Chem. Chem. Phys.* **2005**, *7*, 3297.
(45) Weigend, F.; Häser, M.; Patzelt, H.; Ahlrichs, R. *Chem. Phys. Lett.* **1998**, *294*, 143.